Molecular Crystals and Liquid Crystals

Publication details, including instructions for authors and subscription information:
http://www.tandfonline.com/loi/gmcl20

Transient Light scattering of Ferroelectric Liquid Crystals Enhanced by Adding Ferroelectric Liquid Crystalline Polymers

Manabu Kawasaki [a], Huai Yang [a], Hirotsugu Kikuchi [a] & Tisato Kajiyama [a]

[a] Department of Applied Chemistry, Faculty of Engineering, Kyushu University, 6-10-1 Hakozaki, Higashi-ku, Fukuoka, 812-81, Japan

Version of record first published: 18 Oct 2010

To cite this article: Manabu Kawasaki, Huai Yang, Hirotsugu Kikuchi & Tisato Kajiyama (2002): Transient Light scattering of Ferroelectric Liquid Crystals Enhanced by Adding Ferroelectric Liquid Crystalline Polymers, Molecular Crystals and Liquid Crystals, 381:1, 69-84

To link to this article: http://dx.doi.org/10.1080/713738731

Mol. Cryst. Liq. Cryst., Vol. 381, pp. 69–84

1058-725X/02 $12.00 + .00
DOI: 10.1080/10587250290102116

TRANSIENT LIGHT SCATTERING OF FERROELECTRIC LIQUID CRYSTALS ENHANCED BY ADDING FERROELECTRIC LIQUID CRYSTALLINE POLYMERS

*Manabu Kawasaki, Huai Yang, Hirotsugu Kikuchi, and Tisato Kajiyama**
Department of Applied Chemistry, Faculty of Engineering, Kyushu University, 6-10-1 Hakozaki, Higashi-ku, Fukuoka 812-81, Japan

A side-chain type ferroelectric liquid crystalline polymer (FLCP) was mixed with a low-molecular-weight ferroelectric liquid crystal (LMWFLC) to improve the light switching contrast for the transient light-scattering mode (TSM). Optical transmittance through an optically homogeneous chiral smectic C phase in a FLCP/LMWFLC composite system was observed by a polarizing optical microscope. The transmittance of the transparent state of the composite system upon the application of a d.c. electric field was almost the same in comparison with that of LMWFLC. On the other hand, the light-scattering intensity for the composite system upon the application of an a.c. electric field was somewhat stronger than that for LMWFLC. The enhancing mechanism of the transient light scattering induced by an addition of FLCP to LMWFLC has been discussed through the light switching measurements for free-standing FLC thin films.

Keywords: transient light scattering; ferroelectric; liquid crystal; chiral smectic C phase; liquid crystalline polymer; electro-optical switching

INTRODUCTION

Chiral smectic C(S_C*) liquid crystals exhibit ferroelectricity [1,2] and several novel electro-optical effects with high-response speed due to their spontaneous polarization (P_S) [3–9]. The ferroelectric liquid crystalline (FLC) molecules in a S_C* phase form a helical smectic-layer structure; that

Received 31 January 2002; accepted 19 March 2002.
The materials PEO8EMB and CS1024 were kindly supplied by Idemitsu Kosan Co., Ltd. and Chisso Co., Ltd., respectively.
*Corresponding author. Fax: 81-92-651-5606; E-mail: kajiyama@cstf.kyushu-u.ac.jp

is, the azimuthal angle around the layer normal changes regularly along the same direction with the passing of one layer to another layer, while the tilt angle of the molecular long axes of the FLC molecules is the same relative to the smectic layer normal. The P_S generates in each smectic layer along the direction perpendicular to the plane containing both the molecular long axis and the layer normal (the helical axis of the chiral smectic layer). Therefore, when a d.c. electric field is applied perpendicular to the layer normal, the molecules rotate around the layer normal on the tilt cone so that the direction of P_S agrees with that of the applied electric field. This uniform alignment state of FLC molecules shows a high transmittance because the molecular aggregation state is optically homogeneous. When the polarity of an electric field is reversed, the FLC molecules reorient with the polarization inversion and exhibit a transient light-scattering state. This light-scattering state can be continuously preserved by repetition of the polarization inversion upon applying an a.c. electric field with a proper frequency. Then, the light-scattering state and the transparent one can be switched reversibly by changing to an a.c. field and a d.c electric one alternately. This electro-optical effect of FLC was designated as the transient scattering mode (TSM) by Yoshino et al. [4]. Though TSM can be applied as a bright display with high-speed response characteristics, a higher contrast is further required as a conventional display device. It might be expected that the light-switching contrast of TSM can be improved by increasing the number of light-scattering sources or domains which induce incoherent molecular reorientation during the polarization reverse of an applied electric field.

In this paper, the transient light-scattering characteristics for the composite systems in a ferroelectric phase [ferroelectric liquid crystalline polymer (FLCP)/low-molecular-weight ferroelectric liquid crystal (LMWFLC)] have been investigated. The mechanism of the transient light scattering and the addition effect of FLCP to LMWFLC have also been discussed through electro-optical switching properties.

EXPERIMENTAL

The constituent materials for the composite system are shown in Figure 1. FLCP (PEO8EMB, supplied by Idemitsu Kosan Co., Ltd., Japan) and LMWFLC (CS1024, supplied by Chisso Co., Ltd.) with various ratios were dissolved in acetone and then the composite systems were prepared by a solvent-casting method.

The phase transition behaviors of the composite systems were investigated by differential scanning calorimetry (DSC) and polarizing optical microscopy (POM) studies. The heating and cooling rates for DSC

1) Ferroelectric liquid crystalline polymer

PEO8EMB

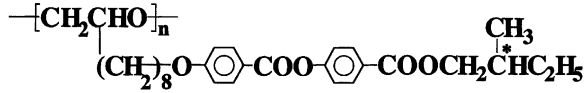

glassy 273 **Sc*** 323 **SA** 347 **Iso. (unit: K)**

$\overline{Mn}$ **: 2100 (GPC, polystyrene standard)**

2) Low-molecular-weight ferroelectric liquid crystal

CS1024 (Mixture)

K 261 **Sc*** 335 **SA** 355 **N*** 363 **Iso.**

Ps: -46.9 nC·cm^{-2}, θ: 25°, Pitch: > 20 μm

(at 298 K)

FIGURE 1 Component materials for the composite system.

measurement and POM observation were 5 and 1 K·min^{-1}, respectively. An S_C* phase was identified by POM observation and P_S measurement. The magnitude of the tilt angle in the S_C* phase was determined from POM observation. Also, the magnitude of P_S was evaluated by a triangular wave-voltage method [10].

Figure 2 shows a schematic diagram of the measurement system of electro-optical properties for the composite systems. The composite system was sandwiched between two ITO (indium-tin oxide)-coated glass substrates. Poly(vinyl alcohol) was coated on the substrate surfaces and rubbed in a uniaxial direction to obtain a homogeneous alignment of FLC molecules. The cell thickness was adjusted to be 12 μm by a poly(ethylene terephthalate) film spacer. A He-Ne laser providing 2 mW at 632.8 nm was used as an incident light. The incident light was transmitted normally to the cell and the transmitted light intensity upon the application of an electric field was measured by a photodiode without any polarizers.

A free-standing FLC film [11,12] was prepared for light-switching measurement. The sample holder of the free-standing film is shown in Figure 3a. A pair of ITO electrodes was attached to the edge of the long side of the hole in the glass plate to apply a voltage in the direction perpendicular to the film normal. The FLC film was drawn by spatula over the rectangular hole as shown in Figure 3b. After an adequate annealing treatment, the smectic layer plane of the FLC aligned parallel to the surface of the FLC film as shown in Figure 3c, that is, the smectic layer normal agrees with the film plane normal. The film thickness was determined by ellipsometry by a senarmont method [13–15]. The experimental setup for measuring the

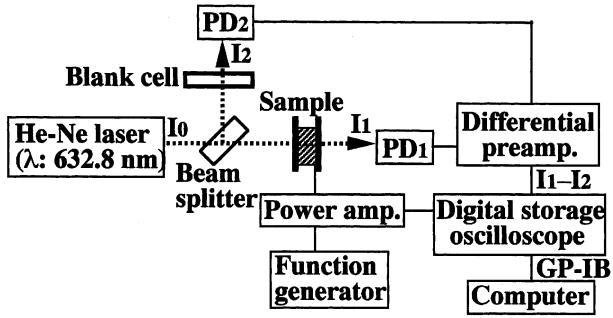

FIGURE 2 Schematic diagram of the measurement system of electro-optical properties for the composite system.

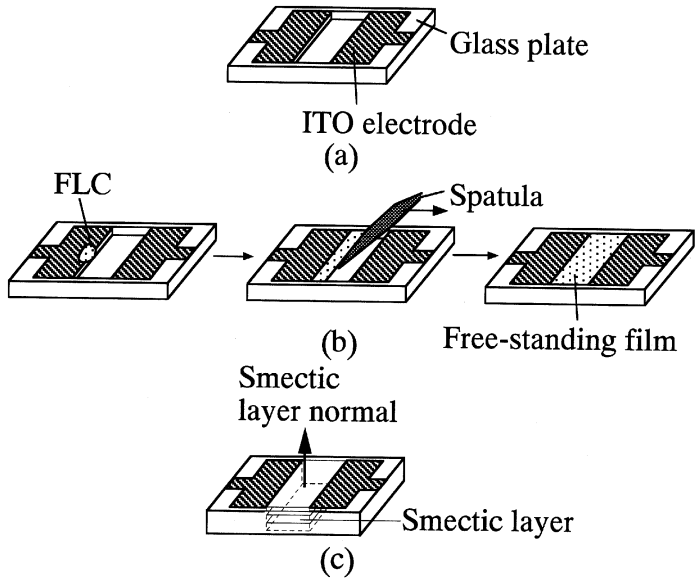

FIGURE 3 Schematic representation of free-standing film; (a) sample holder, (b) preparing method, (c) alignment state.

electro-optical properties of the free-standing FLC film was similar to that for the sandwiched cell. The He-Ne laser beam was incident on the free-standing film at the incident angle of 45° relative to the film normal and the direction of the incident light was set so that the incident plane was parallel to the applied electric field. The incident light was linearly polarized by a polarizer which was set between the light source and the sample. The

polarizing angle of linearly polarized incident light was defined as the angle between the incident plane and the polarization plane.

RESULTS AND DISCUSSION

Aggregation States of the Composite System

The DSC curves of the composite systems (PEO8EMB: FLCP/CS1024: LMWFLC) are shown in Figure 4. The glass transition temperature, Tg, of the composite system was lowered with an increase of the CS1024 fraction

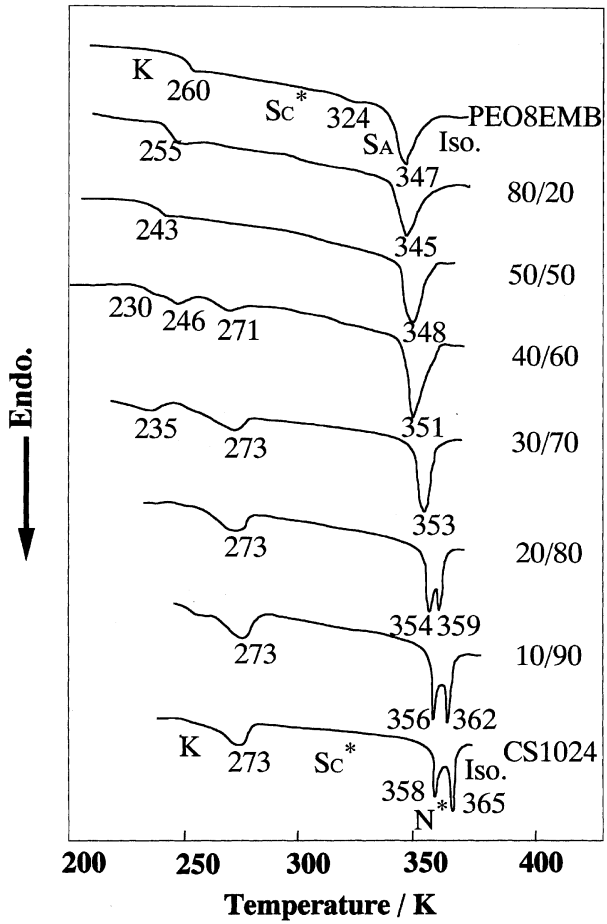

FIGURE 4 DSC curves of the composite system (PEO8EMB/CS1024).

in the PEO8EMB fraction range above 30 wt%. The decrease in Tg might be caused by a plasticizing effect of CS1024 against PEO8EMB. A single endothermic peak due to a mesophase-isotropic phase transition was observed in all DSC curves of the composite systems. This result indicates that the composite systems form a homogeneously mixed mesomorphic phase, and then CS1024 is miscible over the whole concentration range of PEO8EMB in both the isotropic and mesomorphic phase. The POM image of the composite system (PEO8EMB/CS1024 = 10/90 wt%) at 300 K is shown in Figure 5. A striped texture and a fan-shaped one were recognized for the whole concentration range of PEO8EMB. Since the striped texture and the fan-shaped one correspond to the helical structure and the smectic-layer structure, respectively, the POM image apparently indicates the existence of a S_C* phase. Also, in cases where the fraction of PEO8EMB was below 40 wt% the average direction of the optical axis in each fan-shaped texture changed reversibly when the polarity of an applied electric field was reversed. This means that the molecular reorientation was caused by the polarization inversion of the S_C* phase in composite systems with the fraction of PEO8EMB below 40 wt%. In cases where the fraction of PEO8EMB was above 50 wt%, the average direction of the optical axis in each fan-shaped texture did not change in spite of application of an electric field. Furthermore, the spontaneous polarization, P_S, vanished in the case of composite systems with the fraction of PEO8EMB above 50 wt%. These

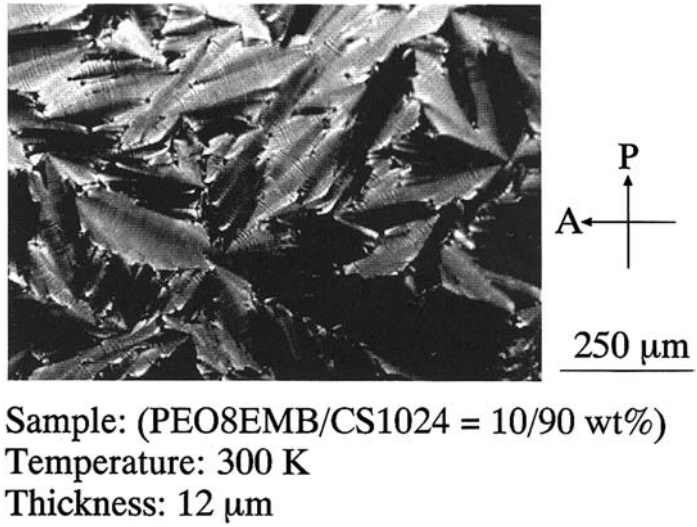

FIGURE 5 POM image of the composite system (PEO8EMB/CS1024).

results indicate that composite systems with the fraction of PEO8EMB above 50 wt% do not exhibit ferroelectricity. The phase diagram of the composite system (PEO8EMB/CS1024) was obtained on the basis of the DSC measurement, the POM observation, and the P_S measurement as shown in Figure 6.

Electro-Optical Properties of the Composite System

The electro-optical properties were measured out for the composite systems in the hatched region of Figure 6, since the composite systems were the optically homogeneous S_C* with a ferroelectric characteristic. Figure 7 shows the light-switching curves for the composite system under the application of an electric field with a rectangular wave form. The composite systems showed a transparent state upon the application of a d.c. electric field in a similar fashion to CS1024. On the other hand, a transient transmittance reduction corresponding to the transient light scattering was found when the polarity of an electric field was reversed as shown in Figure 7. The magnitude of light transmittance for the transparent state was slightly affected by the addition of PEO8EMB to CS1024. The transmittance for the transient-scattering state decreased, that is, the transient-scattering intensity increased with an increase in the fraction of PEO8EMB.

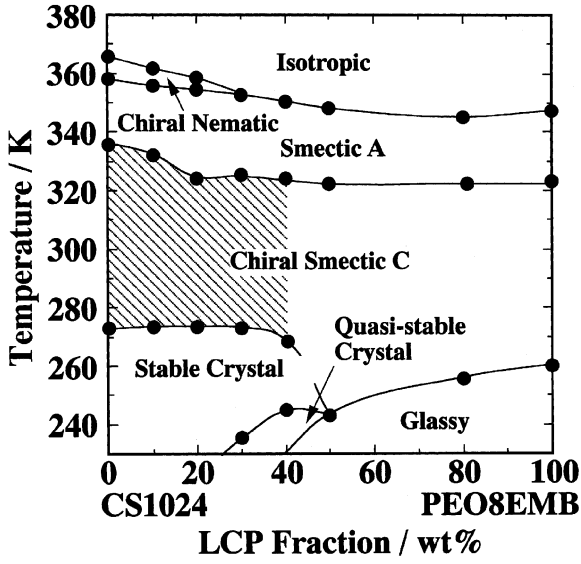

FIGURE 6 Phase diagram of the composite system (PEO8EMB/CS1024).

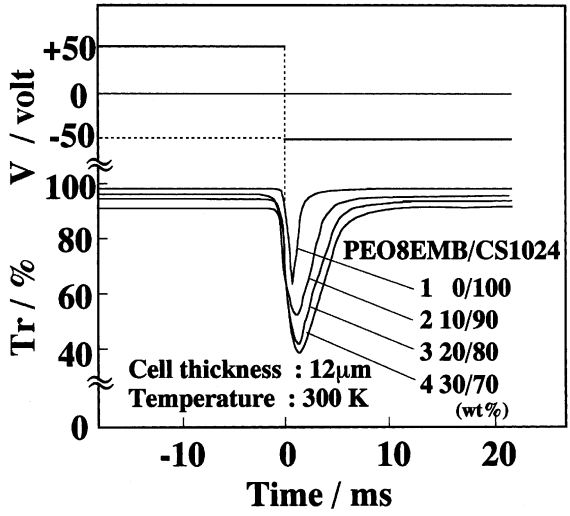

FIGURE 7 Light-switching curves for the composite system (PEO8EMB/CS1024).

In order to normalize the magnitude of transient light-scattering intensity, the degree of transient light scattering τ was used:

$$\tau d = \log(T_2/T_1) \tag{1}$$

where d is the film thickness of the composite system. Also, T_1 and T_2 are the transmittances for the transient light-scattering state and that for the transparent state, respectively. Therefore, the completely turbid state ($\tau d = \infty$) and the completely transparent one ($\tau d = 0$) correspond to the contrast ratios, $T_2T_1 = \infty$ and $T_2T_1 = 1$, respectively.

Figure 8 shows the temperature dependence of τd for the various composite systems. For each curve, τd decreased slightly with an increase of temperature in a temperature range below 320 K and then decreased sharply in a narrow temperature range above 320 K due to a rapid vanishing of ferroelectric property. The magnitude of τd in a temperature range below 320 K increased with an increase of PEO8EMB fraction as shown in Figure 8. This result will be discussed later.

A Possible Mechanism of Transient Light Scattering

Transient light scattering derives from dynamic light scattering being induced by dynamic molecular reorientation. It is expected that the spatial distribution of the refractive index of the FLC should be heterogeneous in the molecular reorientation process. The FLC molecules are optically

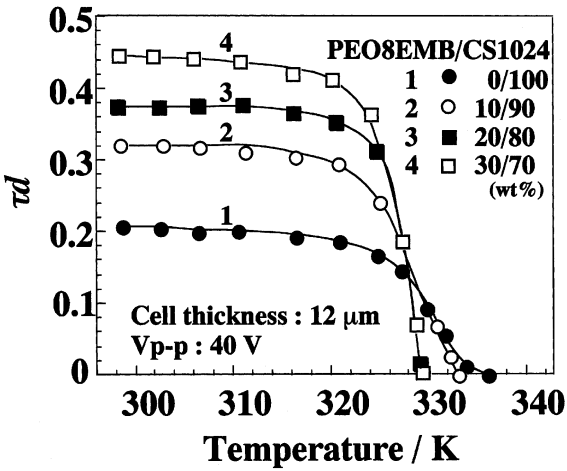

FIGURE 8 Temperature dependence of τ of the composite system (PEO8EMB/CS1024).

homogeneous before and after molecular reorientation because the FLC molecules align uniformly upon the application of a d.c. electric field. Then, if all FLC molecules rotate simultaneously and uniformly, heterogeneity of the refractive index should not be induced. That is to say, the heterogeneous state of the refractive index may arise from the velocity distribution of molecular reorientation. In order to explain the transient light-scattering mechanism, let us consider a change in the refractive index against linearly polarized light n_p when the linearly polarized light is incident perpendicular to the smectic layer normal of FLC. The geometrical relationship between incident light and the FLC molecule is shown in Figure 9a. The x-and z-axes correspond to the propagation direction of the incident light and the smectic layer normal of FLC, respectively. The direction of an applied electric field is parallel to the x-axis. Also, θ and ϕ are the tilt angle of the molecular long axis from the z-axis and the azimuthal angle around the z-axis, respectively. The magnitude of ϕ changes from 0 to π with the constant θ when an applied electric field changes from $+\mathbf{E}$ to $-\mathbf{E}$. The polarizing direction of the transmitted light was parallel to the direction of the molecular long axis in the case of $\phi = 0$, that is, the polarizing angle of the incident light $P = -\theta$. The relationship among n_p and two intrinsic refractive indices, $n_{||}$ and $n_{\perp}$, for linearly polarized light parallel and perpendicular to the director of FLC, respectively, can be formulated from the geometrical relationship between the polarizing direction of the incident light and the direction of the optical axis of the FLC molecule as follows:

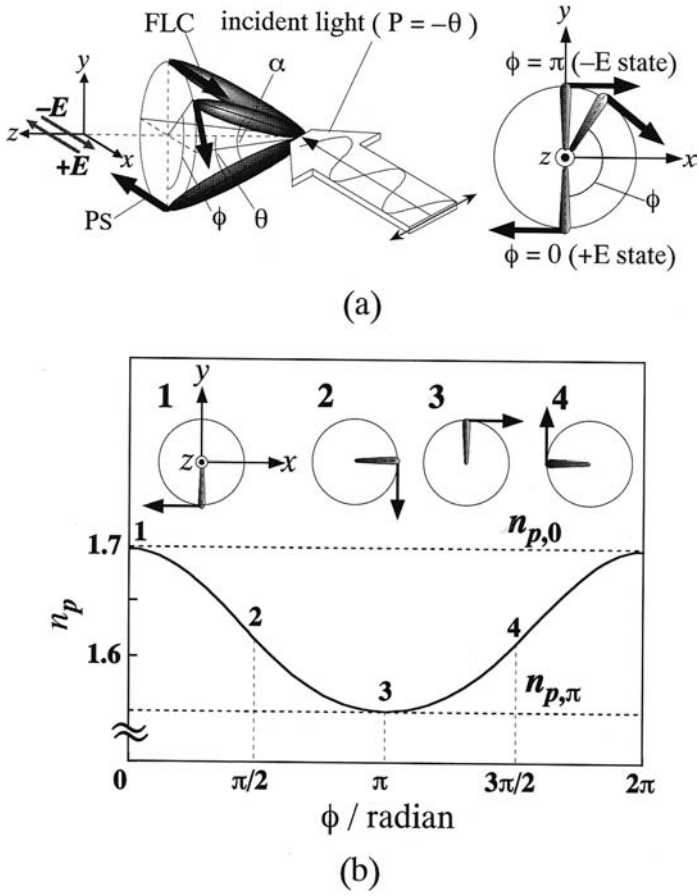

FIGURE 9 Azimuthal angle dependence of n_p.

$$n_p = \frac{n_{||} n_{\perp}}{\sqrt{{n_{||}}^2 \sin^2 \alpha + {n_{\perp}}^2 \cos^2 \alpha}} \tag{2}$$

where α is the angle between the polarizing direction of the transmitted light and molecular long axis at an arbitrary ϕ as given by Equation (3) using θ and ϕ.

$$\alpha = 2 \sin^{-1}\{\sin\theta \sin(\phi/2)\} \tag{3}$$

Also, $n_{p,0}$ and $n_{p,\pi}$ for the cases of n_p at $\phi = 0$ and $\phi = \pi$, respectively, are given by Equations (4) and (5).

$$n_{p,0} = n_{||} \tag{4}$$

$$n_{p,\pi} = \frac{n_{||} n_{\perp}}{\sqrt{{n_{||}}^2 \sin^2\theta + {n_{\perp}}^2 \cos^2\theta}} \tag{5}$$

The calculated values of n_p against ϕ are plotted based on Equations (2) to (5) in Figure 9b. The magnitude of n_p changes sinusoidally from n_p, 0 to n_p, π with the change of ϕ. It seems reasonable to consider that the incoherent molecular reorientation may induce a spatial heterogeneity of the refractive index. If a spatially heterogeneous molecular alignment state shown in Figure 10a is formed by the FLC system due to the velocity distribution of molecular reorientation, the spatial distribution of the average refractive index could be schematically illustrated by Figure 10b.

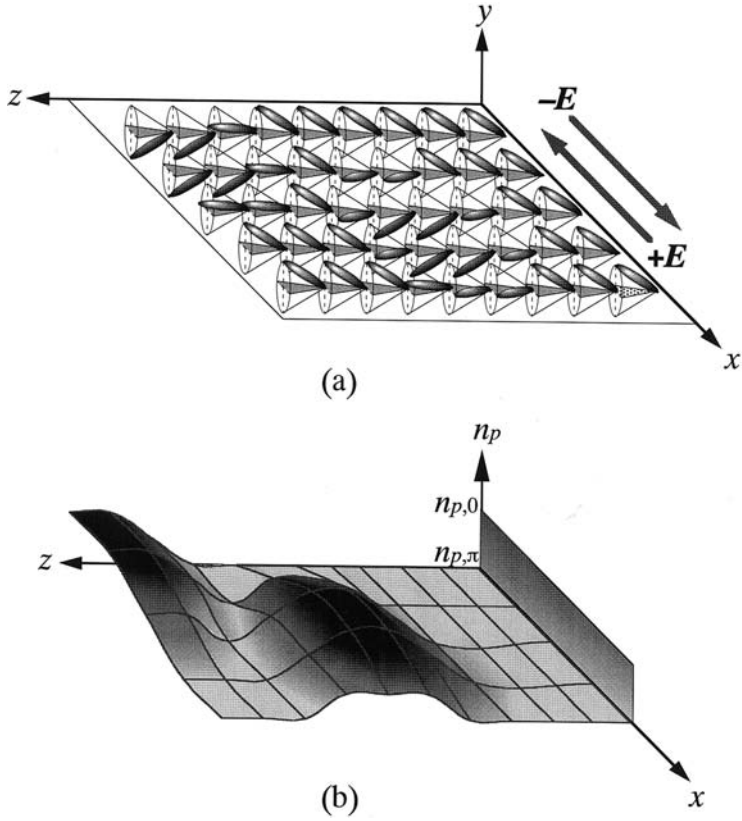

FIGURE 10 Model of mechanism of transient light scattering.

Therefore, then the spatial distribution dimension of the refractive index is comparable to the order of the wavelength of visible light, and the transient light scattering should be observed for the FLC system.

Relationship Between Spatial Distribution of Refractive Index and Transient Light-Scattering Intensity

It is considered from the discussion mentioned above that the magnitude of transient light scattering is governed by the spatial distribution of the refractive index, $n(r, t)$, where $\boldsymbol{r}$ and t are the position in the film and time, respectively. In the case of the linearly polarized incident light with an arbitrary polarizing angle,

$$n(\boldsymbol{r}, t) = \delta n f_\phi(\boldsymbol{r}, t) = n_{p,\min} \tag{6}$$

$$\delta n = n_{p,\max} - n_{p,\min} \tag{7}$$

where $n_{p,\max}$ and $n_{p,\min}$ are the maximum value and the minimum value, respectively, of the refractive index with an arbitrary polarizing angle of incident polarized light. $f_\phi(\boldsymbol{r}, t)$ describes the spatial distribution of n at t during the molecular reorientation and varies in the range $0 \leq f_\phi(\boldsymbol{r}, t) \leq 1$. For example, at the polarizing angle $P = -\theta$, $n_{p,\max} = n_{p,0}$, and $n_{p,\min} = n_{p,\pi}$. Since the δ_n is the difference between $n_{p,\max}$ and $n_{p,\min}$ the magnitude of δn depends on the optical anisotropy of FLC molecules and also the tilt angle of the molecular long axis relative to the smectic layer normal. The Fourier transformation of Equation (6) is analogous to the structural factor used in X-ray diffraction analysis. Therefore, if the spatial profile of $f_\phi(\boldsymbol{r},t)$ is comparable to the wavelength of the incident light and the magnitude of δn is large, the incident light is scattered strongly.

Generally speaking, the fluctuation of molecular motion and the alignment of the FLC molecules near the (FLC/substrate) interface is strongly affected by the interfacial interaction. Therefore, it is reasonable to consider that the interfacial interaction influences the light-scattering properties, especially in the case of the thin cell. However, with respect to the proposed light-scattering model, the effect from the interfacial interaction on the light-scattering properties is neglected. So, the experimental verification of the model was carried out by using a free-standing FLC film for which the area of the (FLC/ITO electrode) interface is as small as possible. Figure 11 shows the polarizing angle dependence of τd for the free-standing FLC films at various temperatures. Each curve shows the minimum value when the polarizing angle is 0 or π. That is, these cases correspond to those when the polarization plane of incident light is parallel to the smectic layer normal or perpendicular to the smectic layer normal, respectively. The polarizing angle at the maximum τ decreased with

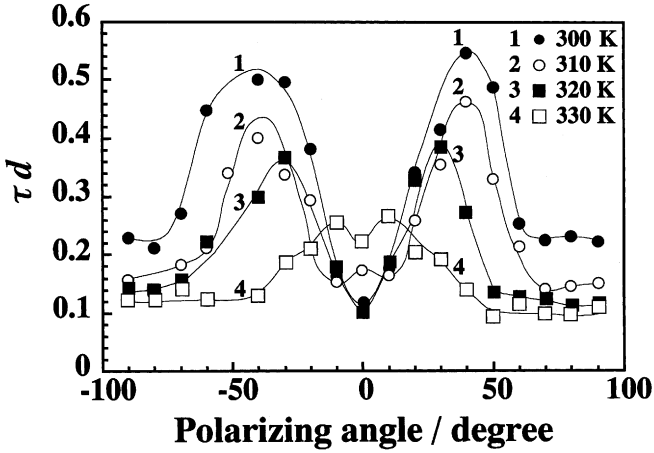

FIGURE 11 Polarizing angle dependence of τ of the free-standing film.

increasing temperature, as discussed below. In the case of the free-standing film, since the transmitted light is refracted as shown in Figure 12, the angle between the propagation direction of the transmitted light in the film and layer normal, Θ, is expressed on the basis of Snell's law,

$$\Theta = \sin^{-1}(\sin 45^\circ / n_{\text{film}}) \tag{8}$$

where n_{film} is the average refractive index of the free-standing film. The optical property was determined by the refractive index against the

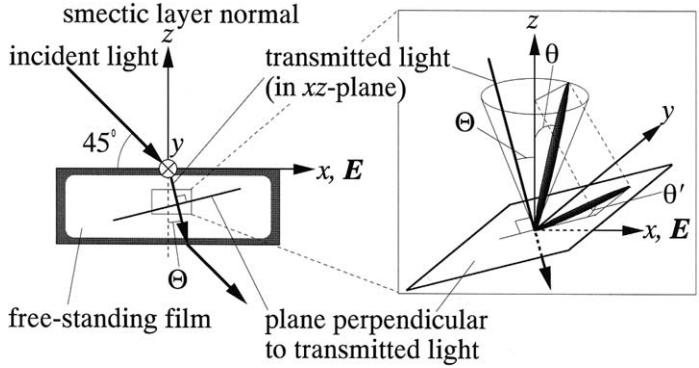

FIGURE 12 Schematic diagram for explaining the apparent tilt angle against transmitted light.

polarizing angle of transmitted light. Since the polarizing direction is perpendicular to the propagation direction of transmitted light, the refractive index is decided by the angle between the polarizing direction of transmitted light and the projection of the molecular long axis toward the plane perpendicular to the propagation direction of transmitted light. The direction of the projected molecular long axis on the plane perpendicular to the propagation direction of transmitted light changes during the polarization inversion. So, the angle variation of electric vector $2\theta'$ in the angle which is determined by tilt angles θ and Θ is expressed as follows:

$$\theta' = \tan^{-1}\left(\frac{\tan\theta}{\sin\Theta}\right) \tag{9}$$

The magnitude of θ' is the apparent tilt angle of the molecular long axis against the transmitted light. The values of θ and θ' at various temperatures are summarized in Table 1. The polarizing angle at the maximum τ agreed well with the magnitude of θ' in Figure 11. So, it apparently indicates that the light-scattering characteristics are governed by the tilt angle, that is, the value of δn, as shown by Equations (2), (4), (5), (6), and (7).

Enhancing Factor for Transient Light-Scattering Intensity of the Composite System

Figure 13 shows the temperature dependence of the tilt angle for the composite system. The tilt angle slightly changed with an increase of the PEO8EMB fraction. This indicates that δn slightly changes by adding PEO8EMB to CS1024. However, τ increased with an increase of the PEO8EMB fraction as shown in Figure 8. This indicates that the magnitude of transient light scattering was governed not by δn but mainly by the change of $f_\phi(r, t)$ for the (PEO8EMB/CS1024) composite system.

Since the reorientation of the side chain of PEO8EMB is restricted because of the coupling with the main chain, it seems reasonable to consider that the locally heterogeneous domain structure is formed in the composite

TABLE 1 Tilt Angle θ and Apparent Tilt Angle θ' at Various Temperatures

Temperature/K	θ/degree	θ'/degree
300	25.0	46.5
310	21.2	41.3
320	16.5	33.9
330	1.8	4.1

$n_{film} = 1.6$

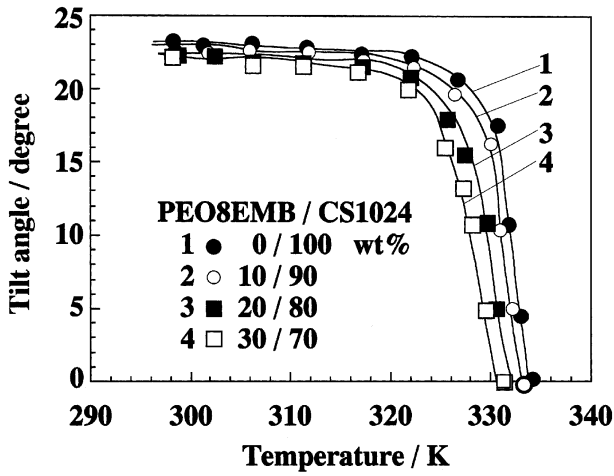

FIGURE 13 Temperature dependence of tilt angle of the composite system (PEO8EMB/CS1024).

system. This locally heterogeneous molecular aggregation state easily induces a time lag with respect to the molecular reorientation of CS1024 during the polarization inversion because the higher viscous region is formed in the vicinity of the PEO8EMB chain in the composite system. Therefore, it is reasonable to conclude that an increase of transient light-scattering intensity may be attributed to an increase of the discontinuous points in the refractive index, of which distribution is comparable to the wave length of the incident light.

CONCLUSION

The composite systems (PEO8EMB/CS1024) showed an optically homogeneous S_C^* phase. The composite systems showed a transparent state upon the application of a d.c. electric field in a fashion similar to LMWFLC. The transient light-scattering intensity increased with an increase of the FLCP fraction. The model of the mechanism of the transient light scattering was proposed under the consideration that the transient light scattering might arise from the variation of the refractive index with a transmitted light during the polarization inversion. The polarizing angle dependence on the degree of the transient light scattering, τ, for the free-standing film was measured to verify the proposed model. The polarizing angle for the maximum τ agreed with the apparent tilt angle of the projected molecular long axis toward the polarizing direction. This result indicates that the tilt angle

is one of the enhancing factors for transient light scattering. It was revealed from the tilt angle measurement that the birefringence of the composite system did not change with an increase of the PEO8EMB fraction. Therefore, the increase of the transient light-scattering intensity might have resulted from the extent of the distribution of the velocity of polarization inversion due to the high viscosity of the main chain of the FLCP.

REFERENCES

[1] Meyer, R. B. (1977). *Mol. Cryst. Liq. Cryst.*, *40*, 33–48.
[2] Meyer, R. B., Liebert, L., Stzelecki, L., & Keller, L. (1975). *J. Phys. Lett.*, *36*, L69–L71.
[3] Clark, N. A., & Lagerwall, S. T. (1980). *Appl. Phys. Lett.*, *36*, 899–901.
[4] Yoshino, K., & Ozaki, M. (1984). *Jpn. J. Appl. Phys.*, *23*, L385–L391.
[5] Yoshino, K., Balakrishnan, K. G., Iwasaki, Y., Uemoto, T., & Inuishi, Y. (1978). *Jpn. J. Appl. Phys.*, *17*, 597–602.
[6] Shelton, J. W., & Shen, Y. R. (1984). *Phys. Rev. Lett.*, *25*, 23–26.
[7] Jakli, A., Bata, L., Buka, A., Eber, N., & Janossy, I. (1985). *J. Phys. Lett.*, *46*, L759–L761.
[8] Jeong, H.-K., Kikuchi, H., & Kajiyama, T. (1997). *Polym. J.*, *29*, 165–170.
[9] Kawasaki, M., Kikuchi, H., & Kajiyama, T. (1996). *Trans. Mat. Res. Soc. Jpn.*, *20*, 303–306.
[10] Miyasato, K., Abe, S., Takezoe, H., Fukuda, A., & Kuze, E. (1983). *Jpn. J. Appl. Phys.*, *22*, L661–L667.
[11] Young, C. Y., Pindak, R., Clark, N. A., & Meyer, R. B. (1978). *Phys. Rev. Lett.*, *40*, 773–776.
[12] Rosenblatt, C., Meyer, R. B., Pindak., & Clark, N. A. (1979). *Phys. Rev. Lett.*, *42*, 1220–1223.
[13] Bahr, Ch., & Fliegner, D. (1992). *Rev. Lett. A*, *46*, 7658–7661.
[14] Amador, S. M., & Pershan, P. S. (1990). *Rev. Lett. A.*, *41*, 4326–4329.
[15] Aspnes, D. E., & Studna, A. A. (1975). *Appl. Opt.*, *14*, 220–228.